J. Am. Soc. Mass Spectrom. (2018) 29:1611–1626
DOI: 10.1007/s13361-018-1972-4

RESEARCH ARTICLE

On the Kendrick Mass Defect Plots of Multiply Charged Polymer Ions: Splits, Misalignments, and How to Correct Them

Thierry N. J. Fouquet,[1] Robert B. Cody,[2] Yuka Ozeki,[3] Shinya Kitagawa,[3] Hajime Ohtani,[3] Hiroaki Sato[1]

[1]Research Institute for Sustainable Chemistry, National Institute of Advanced Industrial Science and Technology (AIST), Tsukuba, Japan
[2]JEOL USA, Inc., Peabody, USA
[3]Graduate School of Engineering, Life Science and Applied Chemistry, Nagoya Institute of Technology, Nagoya, Japan

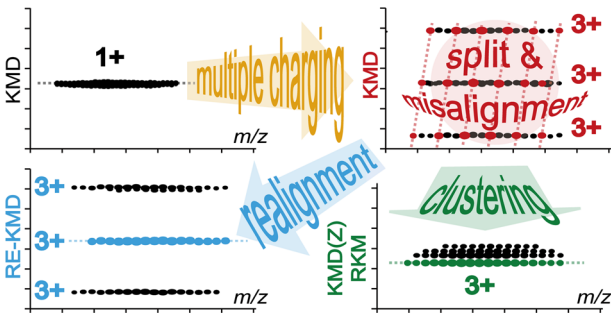

Abstract. The Kendrick mass defect (KMD) analysis of multiply charged polymeric distributions has recently revealed a surprising isotopic split in their KMD plots—namely a 1/*z* difference between KMDs of isotopes of an oligomer at charge state *z*. Relying on the KMD analysis of actual and simulated distributions of poly(ethylene oxide) (PEO), the isotopic split is mathematically accounted for and found to go with an isotopic misalignment in certain cases. It is demonstrated that the divisibility (resp. indivisibility) of the nominal mass of the repeating unit (R) by *z* is the condition for homolog ions to line up horizontally (resp. misaligned obliquely) in a KMD plot. Computing KMDs using a fractional base unit R/*z* eventually corrects the misalignments for the associated charge state while using the least common multiple of all the charge states as the divisor realigns all the points at once. The isotopic split itself can be removed by using either a new charge-dependent KMD plot compatible with any fractional base unit or the remainders of KM (RKM) recently developed for low-resolution data all found to be linked in a unified theory. These original applications of the fractional base units and the RKM plots are of importance theoretically to satisfy the basics of a mass defect analysis and practically for a correct data handling of single stage and tandem mass spectra of multiply charged homo- and copolymers.

Keywords: Kendrick mass defect, Charge state, Multiply charged ions, Polymer, Fractional base unit, Poly(ethylene oxide), KMD, Remainders of Kendrick mass, High-resolution mass spectrometry

Received: 16 January 2018/Revised: 17 April 2018/Accepted: 18 April 2018/Published Online: 11 May 2018

Introduction

A Kendrick mass defect (KMD) analysis [1–6] has become a powerful visualization and data processing tool for the mass spectra of natural [7–10] and synthetic polymers [11]. The historical KMD analysis first consists of a change of basis from the IUPAC mass scale (based on $m(^{12}C) = 12$ a.u.) to a Kendrick mass (KM) scale based on the nominal mass of CH_2 set at 14 a.u. (Eq. (1)) [12], particularly well-suited for carbonaceous samples such as petroleum [13].

$$\mathrm{KM} = m/z \cdot \frac{14}{14.0157} \quad (1)$$

This founding formula has been kept unchanged since its introduction by Kendrick 50 years ago and its use for the so-

Electronic supplementary material The online version of this article (https://doi.org/10.1007/s13361-018-1972-4) contains supplementary material, which is available to authorized users.

Correspondence to: Thierry Fouquet; *e-mail:* thierry.fouquet@aist.go.jp

called KMD analysis proposed in the 1980s [14, 15]. In its modified version for polymer ions proposed by Sato et al. 4 years ago, the repeating unit of a polymer backbone (noted R) is used as the base unit by arbitrarily setting its mass at the nearest integer (e.g., ethylene oxide (EO) at 44.0262 in the IUPAC scale set at 44) and other masses are re-calculated based on this new reference [11]. KMs become a function of R noted KM(R):

$$\mathrm{KM(R)} = m/z \cdot \frac{\mathrm{round(R)}}{\mathrm{R}} \quad (2)$$

Second, the difference between the *nominal* and *exact* Kendrick masses—known as Kendrick mass defect (or mass excess as recently suggested to avoid confusion with the physical definition of mass defect [16])—is evaluated as it contains information about the elemental composition of the species.

$$\mathrm{KMD(R)} = \mathrm{round(KM(R))} - \mathrm{KM(R)} \quad (3)$$

Homologous polymer ions (e.g., congeners of a given distribution carrying the same end groups and adducted ion) have identical KMD and line up horizontally in the associated KMD plot (KMD as a function of *m*/*z* or the nominal KM noted NKM, cf. Glossary in the Supporting Information).

This simple property turns into a compositional mapping for the complex mass spectra of polymeric samples since a full distribution in a mass spectrum is plotted as a set of packed lines in the KMD plot with one line per isotopic composition (mainly $^{13}C_n$). The KMD plot from the mass spectrum of a blend of homopolymers carrying the same repeating unit but different chain ends displays several sets of packed horizontal lines with one set per distribution [11]. Tandem mass spectra of homopolymers are similarly turned into a set of lines with one line per product ion series [17]. On the contrary, the presence of another repeating unit (e.g., blend of different homopolymers) is readily detected through the alignment of points along an oblique direction [11]. The mass spectrum of a copolymer carrying two or three repeating units is displayed as a scatter plot with at least two alignments (e.g., horizontal and oblique) in a KMD plot computed with one of the co-monomers as the base unit [18–21].

A second breakthrough has been proposed a year ago with the introduction of the "resolution-enhanced KMDs" computed using a "fractional base unit" [22] noted R/X with X being a positive integer:

$$\mathrm{X} > 1, \quad \mathrm{KM(R,X)} = m/z \cdot \frac{\mathrm{round(R/X)}}{\mathrm{R/X}} \quad (4)$$

KMs—now function of the repeating unit R and the divisor X—computed with the counter-intuitive base unit R/X are producing KMD plots capable of separating ion series in a high and controllable extent as never reported before [23, 24]. Resolution-enhanced KMD plots are also compatible with high-mass and/or low-resolution datasets normally unsuited for the "regular" KMD analysis (i.e., with R as the base unit, X = 1) [25]. KMDs and RE-KMDs have been used in previous articles as abbreviations for the regular and resolution-enhanced KMD analyses. To avoid the multiplication of acronyms (cf. Glossary in the Supporting Information), the full names will be used in the text while KMD(R) and KMD(R,X) will be used in equations to distinguish the regular and resolution-enhanced outputs, respectively.

With unrivaled capabilities for the analysis of polymers, mass spectra have been extensively recorded using devices equipped with a matrix-assisted laser desorption ionization (MALDI) ion source [26–28]. The formation of singly charged ions mainly is a well-known feature of the MALDI process [29, 30] and the KMD plots of polymer ions reported in the literature are consequently for singly charged distributions only. However, Cody et al. very recently reported on the KMD analysis of multiply charged polymer ions generated by a paper spray ion source [31] and pointed out that the associated KMD plots exhibits a surprising "isotopic split." A polymeric distribution at charge state *z* is indeed displayed as *z* clear lines spaced out by approximately 1/*z* instead of a packed set of lines at charge state 1+. Such unique feature provides the charge state of a series at first sight by counting the number of horizontal lines in the full-scale KMD plot. It also allows a seemingly clear selection of points using appropriate software in a so-called grouping mode (filtering of points from the KMD plot to get the associated peaks in the mass spectrum).

Multiple charging might be a drawback complicating a mass spectrum but reversely allows large species of high molecular weight to be detected in a low mass range and might overcome the restriction of mass spectrometry to low molecular weight polymers [32]. Being an advantage or a pitfall, multiple charging is a feature of the electrospray ion source (ESI) and all its variations of common use for polymers. Counting on an increasing use of the KMD analysis of mass spectra from polymers recorded using such ion sources, the KMD analysis of multiply charged ions had thus to be thoroughly explored to exhaustively describe its features and biases with a satisfactory mathematical framework.

A careful inspection of the KMD plot computed from multiply charged distributions revealed indeed an unexpected isotope misalignment accompanying the isotopic split, i.e., homologs of a given distribution aligning along an oblique axis instead of horizontally. Simple mathematics are proposed to account for this misalignment found to depend on the repeating unit and the charge state. A way to correct the isotope misalignment preserving the informative isotopic split is then proposed by using the concept of a fractional base unit R/X. The new notion of "charge-dependent KMD," its resolution-enhanced counterpart, and the "remainders of KM" [33] (noted RKM, cf. Glossary in the Supporting Information) successfully remove the isotopic split itself, clustering the split lines into a packed cloud. A final mathematical demonstration combines the regular KMDs, the resolution-enhanced KMDs, and the RKMs into a single equation while two applications of this

unified theoretical background are proposed with the data processing of single stage and tandem mass spectra.

Experimental

Chemicals and Materials

(H, OH)-ended poly(ethylene oxide) 3400 g mol^{-1} (PEO 3400) and (H, OH)-ended triblock poly(ethylene-oxide-*block*-propylene oxide-*block*-ethylene oxide) 2000 g mol^{-1} 12% EO (P(EO-*b*-PO-*b*-EO) 2000) were purchased from Sigma-Aldrich (St. Louis, MO) for paper spray experiments while (H, OH)-ended PEO 6000 g mol^{-1} (PEO 6000) was from Serva Electrophoresis (Heidelberg, Germany) for ESI tandem mass spectrometry (ESI-CAD). Chemicals were used as received without purification. Paper triangles used for paper spray experiments were cut from chromatography paper (1 CHR, Whatman International Ltd., Maidstone, UK). (H, OH)-ended PEO oligomers (degree of polymerization 70 and 80 to 85) have also been simulated at charge states $z = 1+$ to $z = 6+$ using the mass calculator implemented in Mass Mountaineer v. 3.5 (RBC Software, Portsmouth, NH) with ^{12}C and $^{13}C_{x=1-7}$ isotopes to check at the validity of the mathematical formulas prior to their use for actual datasets.

Mass Spectrometry

Paper spray mass spectra were recorded using a single-stage reflectron time-of-flight mass spectrometer with an atmospheric pressure interface (AccuTOF-DART, JEOL USA, Inc., Peabody, MA) [31]. The mass spectrometer was equipped with a Direct Ionization in Real Time (DART-SVP) ion source (IonSense LLC, Saugus, MA) and a prototype paper spray ion source. A 2 μL volume of dissolved polymer (1 to 2 μL of neat liquid polymer in 300 μL of methanol) was applied to a fresh paper triangle for each sample measured. Ten to twenty microliters of methanol were additionally deposited to the paper triangles before starting the analysis. Data were acquired by using Mass Center™ software (JEOL Ltd., Tokyo, Japan). TSS Unity™ (Shrader Software Solutions, Detroit, MI) was used for mass calibration, spectral averaging, and background subtraction.

ESI-CAD mass spectra were recorded using a Synapt G2 HDMS (Waters, Milford, MA) equipped with an electrospray ion source in infusion mode. PEO 6000 dissolved in acetonitrile/water 1/1 at 0.1 mg mL^{-1} was introduced using a microsyringe pump (11 Puls, Harvard Apparatus, Holliston, MA) operated separately at a flow rate of 20 μL min^{-1}. Instrument control, data acquisition, and data processing of all experiments were achieved using MassLynx v. 4.1 provided by Waters.

KMD Analysis

KMD plots were computed using msRepeatFinder version 2.0 RC3 (JEOL), Mass Mountaineer, and Excel spreadsheet program with Visual Basic for Applications (VBA) coding for a maximal flexibility (msRepeatFinder v.2.0 does not tolerate manual entries of base unit inferior to 1 and Mass Mountaineer v. 3.5 does not compute RKM plots). The base unit used for the calculation of "regular" and "resolution-enhanced" KMD is a fraction of R noted R/X with X being an integer (X = 1 for a regular KMD plot, X > 1 for a resolution-enhanced KMD plot, cf. introduction for the formulas). At the time of writing, Mass Mountaineer is the only software incorporating the "fractional base unit" option in its mass defect analysis tab with no need for a manual entry (the user directly types the value of X). For the RKM plots, RKMs were computed using $RKM(Y) = \left\{ Y \cdot {}^{KM}/_{(round(R))} \right\}$ with Y a multiplier set at the charge state to be clustered or any integer value (positive or negative, vide infra) and {} being the fractional part function defined as {x} = x − floor(x) [33]. A KMD plot (resp. RKM plot) displays the KMDs of the oligomeric adducts (resp. RKMs) as a function of their *m*/*z* using a three-dimensional "bubble chart" where each disk expresses a data triplet (*m*/*z*, KMD, or RKM, abundance via the size of the disk).

Results and Discussions

Preliminary Considerations: Split and Misalignments of Isotopes

The paper spray mass spectrum of PEO 3400 is depicted in Figure 1a and exhibits extensive multiple charging with polymeric chains adducted by three to six sodium cations (charge states 3+ to 6+ assigned by checking at the mass difference between consecutive isotopes) [31]. The regular KMD plot calculated with EO as the base unit is depicted in Figure 1b and displays several sets of horizontal lines assigned to the four distributions at the four charge states. It illustrates the "isotopic split" with the triply charged series ($z = 3$) being formed of three main lines in the highest *m*/*z* range (spaced by $\sim 1/z = 0.33$, orange arrows) and the 4+, 5+, and 6+ series being formed of four, five, and six main lines in the low *m*/*z* range (spaced by ~ 0.25, ~ 0.2, and ~ 0.17, respectively). A charge state distribution is thus evaluated within a minute by counting the number of lines with no additional data processing. As an obvious pitfall discussed more in details later, all the charge states share one common line at a KMD value close to 0 (not strictly identical, KMD(3+) ~ − 0.0217, KMD(4+) ~ − 0.0222, KMD(5+) ~ − 0.0226, KMD(6+) ~ − 0.0228) and close to the expected single line for a singly charged distribution (KMD(1+) ~ 0.0229).

A filtered mass spectrum of a part of the 4+ series is depicted in Figure 1c using data extracted from the KMD plot (grouping mode in msRepeatFinder, blue solid square). Several isotopes have been grouped denoting a limited separating power but the main four peaks are all spaced by ~ 11.01 which corresponds to the expected mass difference for a PEO at charge state $z = 4$ (EO/4 = 44.0262/4 = 11.0066, inset in Figure 1c). Extracting points horizontally aligned from the 3+ series (Figure 1d, blue dotted square), the main peaks are now

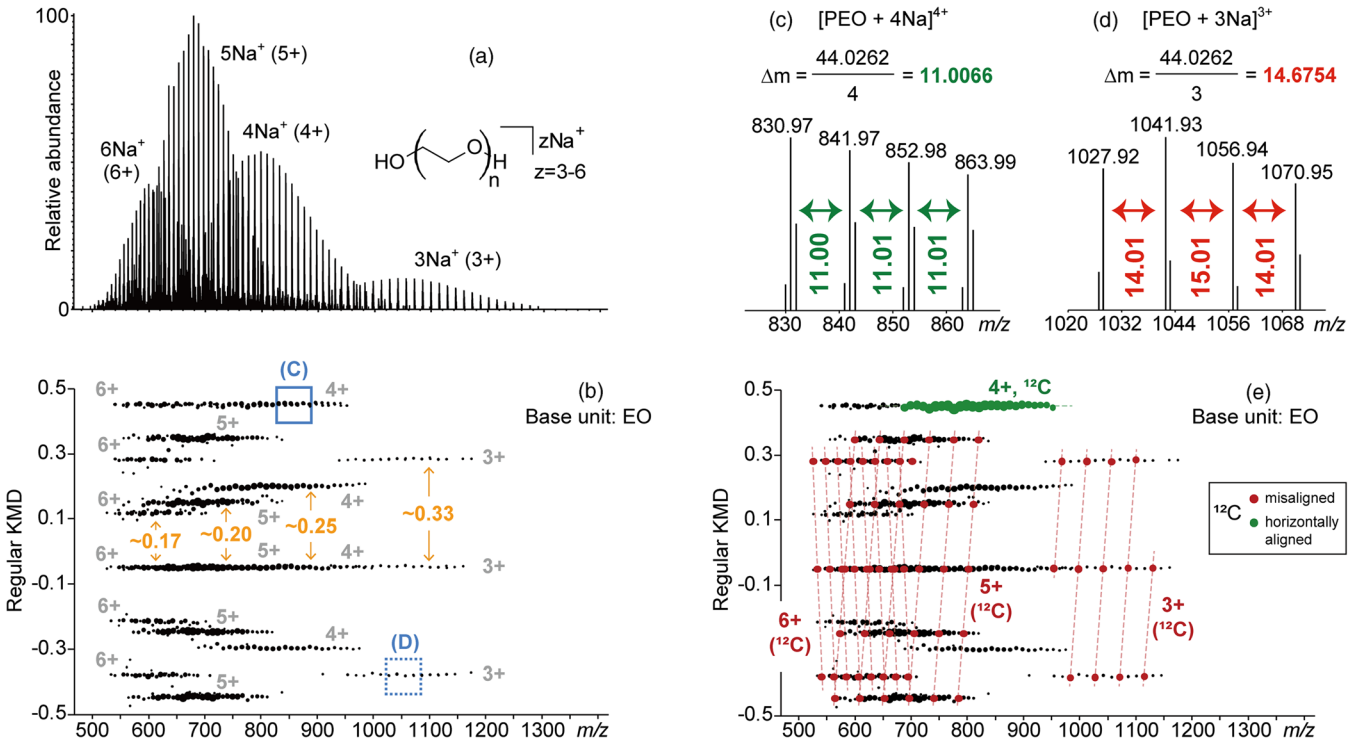

Figure 1. (**a**) Paper spray mass spectrum of PEO 3400. (**b**) Regular KMD plot (base unit: EO). (**c**, **d**) Filtered mass spectra using partial data extracted from the 4+ and 3+ series (blue lines). (**e**) Regular KMD plot with ^{12}C peaks of the 3+/5+/6+ and 4+ series colored in red (misaligned) and green (horizontally aligned), respectively

spaced by 14.01 and 15.01 alternatively, which differs from the expected mass difference between consecutive triply charged homologs (EO/3 = 44.0262/3 = 14.6754, inset in Figure 1d). In spite of a horizontal alignment in the KMD plot, the extracted points have different isotopic compositions (called hereafter isotopologues, e.g., $m/z(n+1,\ ^{13}C_1) - m/z(n,\ ^{12}C) = 15.0087$), $m/z(n+1,\ ^{12}C) - m/z(n,\ ^{13}C_2) = 14.0087$).

To better emphasize this pitfall, the first peaks of the isotopic patterns of every oligomer (referred to as ^{12}C) have been highlighted in the KMD plot of PEO for the four charge states 3+ to 6+ (Figure 1e). The ^{12}C peaks of the 4+ series (in green) have the same KMD and line up horizontally in agreement with the basics of a KMD analysis [11]. On the opposite, the 3+, 5+, and 6+ oligomers surprisingly depart from the expected alignments. The ^{12}C species are aligned along *oblique* directions in lieu of the regular horizontal direction (red points and dashed red lines), positioned on one of the three or five main lines alternatively. In other words, the 3+, 5+, and 6+ ^{12}C species *do not* have the same KMD value if calculated with EO as the base unit while isotopologues line up horizontally. This result is in contradiction with the founding postulate of the KMD analysis of polymer ions claiming that species differing by a number of base units only possess the same KMD value (spread along the *x*-axis) while isotopologues spread vertically.

This "isotopic misalignment" is not detrimental to the visualization of data in the KMD plot—from a practical point of view without considering the isotopes, PEO oligomers are lining up horizontally and the charge states are readily evaluated. However, it reveals from a theoretical point of view that the repeating unit of a homopolymer might not be a satisfactory base unit for the KMD analysis in the case of multiple charging. It is also problematic for the grouping mode (i.e., selecting points from the KMD plot to get the associated peaks in the mass spectrum) since the points forming a given line have a different isotopic composition. Pursuing the development of the mathematical framework recently proposed for the KMD analysis using fractional base units [23, 25, 34], the next two sections deal with the origin of (a) the isotopic split and (b) the isotopic misalignments.

Mathematical Framework to Account for the Isotopic Split

The isotope distribution of an oligomeric adduct is mainly arising from the ^{13}C isotopes. At charge state $z = 1$, the difference between the KMs of the ^{12}C point and its first ^{13}C isotope is:

$$\Delta KM_{^{13}C,^{12}C}(R,1) = \Delta m_{^{13}C,^{12}C} \cdot \frac{\mathrm{round}(R)}{R} \tag{5}$$

with $\Delta m_{^{13}C,^{12}C} = 1.003355$ in the IUPAC scale ($m_{^{12}C} = 12.0000$, $m_{^{13}C} = 13.003355$). At a charge state z, Eq. (5) is transposed as follows:

$$\Delta KM_{^{13}C,^{12}C}(R,z) = \frac{\Delta m_{^{13}C,^{12}C}}{z} \cdot \frac{\mathrm{round}(R)}{R} = \frac{\Delta KM_{^{13}C,^{12}C}(R,1)}{z} \tag{6}$$

Coming to mass defects, the relationship between $\Delta KMD_{^{13}C,^{12}C}(R,z)$ and $\Delta KMD_{^{13}C,^{12}C}(R,1)$ is not as

straightforward as $\Delta KMD_{13C,12C}(R,z) = \Delta KMD_{13C,12C}(R,1)/z$ but would be favorably developed to account for the isotopic split. At charge state $z = 1$, $\Delta KMD_{13C_1,12C}(R,1)$ is decomposed as follows:

$$\begin{aligned}&\Delta KMD_{13C_1,12C}(R,1) \\ &= NKM_{13C}(R,1) - KM_{13C}(R,1) - (NKM_{12C}(R,1) - KM_{12C}(R,1)) \\ &= \Delta NKM_{13C,12C}(R,1) - \Delta KM_{13C,12C}(R,1)\end{aligned} \tag{7}$$

As a founding property, $\Delta NKM_{13C,12C}(R,1) = 1$ whatever the chemically acceptable repeating unit R since ${}^{round(R)}/_{R} \sim 1$ and $\Delta m_{13C,12C} \sim 1$. At a given charge state z, the difference between the KMDs of ^{12}C and ^{13}C isotopes becomes:

$$\begin{aligned}&\Delta KMD_{13C,12C}(R,z) \\ &= \Delta NKM_{13C,12C}(R,z) - \Delta KM_{13C,12C}(R,z)\end{aligned} \tag{8}$$

Contrary to the case of $z = 1$, $\Delta NKM_{13C,12C}(R,z)$ could be 0, 1, or 2 depending on the charge state, the repeating unit, and the degree of polymerization owing to the rounding function. Being an integer, the uncertainty about $\Delta NKM_{13C,12C}(R,z) = \{0,1,2\}$ is not detrimental to the current set of equations since the KMD dimension is focused on the fractional part of masses. By advantageously adding/subtracting $\Delta NKM_{13C,12C}(R,1)/z$, Eq. (8) is then modified in:

$$\begin{aligned}&\Delta KMD_{13C_1,12C}(R,z) \\ &= \frac{\Delta NKM_{13C,12C}(R,1)}{z} - \frac{\Delta KM_{13C,12C}(R,1)}{z} - \frac{\Delta NKM_{13C,12C}(R,1)}{z} (\pm \text{integer})\end{aligned} \tag{9}$$

Considering that $\Delta NKM_{13C,12C}(R,1)/z - \Delta KM_{13C,12C}(R,1)/z = \Delta KMD_{13C,12C}(R,1)/z$ and $\Delta NKM_{13C,12C}(R,1) = 1$ in Eq. (9), it provides the targeted relationship between $\Delta KMD_{13C,12C}(R,z)$ and $\Delta KMD_{13C,12C}(R,1)$:

$$\begin{aligned}&\Delta KMD_{13C_1,12C}(R,z) \\ &= \frac{\Delta KMD_{13C,12C}(R,1)}{z} - \frac{1}{z} (\pm \text{integer})\end{aligned} \tag{10}$$

Equation (10) mathematically describes the so-called isotopic split experimentally observed in the KMD plots of multiply charged ions (Figure 1) [31] and originating from the term "$1/z$," itself found to arise from the value of $\Delta NKM_{13C,12C}(R,1)$ always equal to unity. A few numerical examples are provided in Table 1 with a simulated (H, OH)-PEO 70-mer at charge states 1+ to 3+ and $^{12}C/^{13}C_{1,2}$ isotopes. The quantity $\Delta KMD_{13C_{X+1},13C_X}(EO,z) - \frac{\Delta KMD_{13C_{X+1},13C_X}(EO,1)}{z}$ is equal to $-\frac{1}{z}$ ($= -0.5$ and -0.333 with $z = 2, 3$) in the four cases listed as a support to the validity of Eq. (10). Additional examples are listed in Table S1 in the Supporting Information with charge states $z = +1$ to $+6$ and $^{13}C_{1-6}$ isotopes highlighting the +/− integer uncertainty of no consequence due to the aliasing of the KMD plot [34].

Mathematical Framework to Account for the Misalignments

The previous section rationalized the isotopic split in the KMD plots of multiply charged ions and $\Delta KMD_{13C,12C}(R,z)$ was the function of choice to be derived. This isotopic split might be accompanied by an isotopic misalignment depending on the charge state. Consecutive homolog peaks of a given ion series at a given charge state may not line up horizontally despite an identical composition modulo R. Considering two consecutive oligomers (noted n-mer and $(n+1)$-mer) of the same isotopic composition at a charge state z, the appropriate function to be derived is $\Delta KMD_{n-mer,\ (n+1)-mer}(R,z)$. The difference between their mass-to-charge ratios is:

$$m_{(n+1)-mer}/z - m_{n-mer}/z = \frac{R}{z} \tag{11}$$

The difference $\Delta KM_{n-mer,\ (n+1)-mer}(R,z)$ is then calculated using Eq. (11) and the definition of KM (Eq. (2)) [11]:

$$\Delta KM_{n-mer,(n+1)-mer}(R,z) = \frac{R}{z} \cdot \frac{round(R)}{R} = \frac{round(R)}{z} \tag{12}$$

Using the same decomposition as in the previous section (Eq. (8)), $\Delta KMD_{n-mer,\ (n+1)-mer}(R,z)$ is derived as follows:

$$\begin{aligned}&\Delta KMD_{n-mer,(n+1)-mer}(R,z) \\ &= \Delta NKM_{n-mer,(n+1)-mer}(R,z) - \Delta KM_{n-mer,(n+1)-mer}(R,z)\end{aligned} \tag{13}$$

For a correct isotopic alignment to be achieved, $\Delta KMD_{n-mer,\ (n+1)-mer}(R,z) = 0$ (e.g., the same KMD for two consecutive oligomers of the same isotopic composition). Using Eq. (13), it means $\Delta NKM_{n-mer,\ (n+1)-mer}(R,z) = \Delta KM_{n-mer,\ (n+1)-mer}(R,z)$. Since $\Delta NKM_{n-mer,\ (n+1)-mer}(R,z)$ is an integer by definition of NKM, a *necessary and sufficient condition* for the isotopes to be correctly aligned horizontally simply consists in:

$$\Delta KM_{n-mer,(n+1)-mer}(R,z) = \frac{round(R)}{z} = \text{integer} \tag{14}$$

In other words, if the rounded value of the repeating unit is divisible by the charge state z, the isotope distributions of the oligomers at the given charge state will be correctly aligned.

Table 1. $\Delta KMD_{^{13}C_{X+1},^{13}C_X}(EO,z)-\frac{\Delta KMD_{^{13}C_{X+1},^{13}C_X}(EO,1)}{z}$ Computed from a simulated (H, OH)-PEO 70-mer at charge states 1+, 2+, and 3+ with ^{12}C and $^{13}C_{1,\,2}$ isotopes (full table with charge states 1+ to 6+ and $^{13}C_{1-6}$ isotopes in the Supporting Information, Table S1)

	$z=1$		$z=2$		$z=3$		$\Delta KMD_{^{13}C_{x+1},^{13}C_x}(EO,z)-\frac{\Delta KMD_{^{13}C_{x+1},^{13}C_x}(EO,1)}{z}$		
Isotope	*m/z*	KMD	*m/z*	KMD	*m/z*	KMD	$z=1$	$z=2$	$z=3$
^{12}C (=$^{13}C_0$)	3122.84	0.023	1572.91	0.024	1056.27	0.357	–	–	–
$^{13}C_1$	3123.84	0.020	1573.41	−0.478	1056.61	0.023	−0.003	−0.500	−0.333
$^{13}C_2$	3124.84	0.018	1573.92	0.021	1056.94	−0.312	−0.003	0.500 (=−0.500–1)	−0.333

Otherwise, monoisotopic peaks will line up along an oblique direction producing the so-called isotopic misalignment. Note that the condition defined by Eq. (14) is always true for $z=1$ (singly charged state) by definition of the function "round()" (cf. Glossary in the Supporting Information). Since the KMD plots have been used exclusively for singly charged series from (mainly) MALDI data so far, it accounts for the absence of any article dealing with such isotopic misalignments in the literature.

The divisibility (R/z = integer) and indivisibility (R/z = non-integer) of EO by the charge states $z=1$–6 are listed in Table 2 and found to match the actual isotopic misalignment (red values and red points, $z=3$, 5, 6) or correct horizontal alignment (green values and green points, $z=4$) displayed in Figure 1. To further check at the validity of the mathematical background, the KMD plots of simulated oligomers of PEO at charge states $z=+1$ to +6 are depicted in Fig. S1. Misalignments are observed for the 3+, 5+, and 6+ series and $\frac{round(EO)}{z=3,5,6}$ are non-integers while the 1+, 2+, and 4+ ion series are correctly aligned and $\frac{round(EO)}{z=1,2,4}$ are integers in perfect agreement with Eq. (14). Results would be extended to any other repeating unit as well as negative charge states by using the absolute value of the charge states.

The isotopic misalignment in the KMD plots of multiply charged ions arises from the indivisibility of the rounded repeating unit by the charge state. It is thus associated with the choice of the repeating unit itself as the base unit for the calculation of the Kendrick masses. If this choice is straightforward in many cases, a very recent breakthrough has been made using a fraction of the repeating unit (i.e., R/X with X being a positive integer) which offers unique features such as an improved separation of isotopes or the deconvolution of overlapping series in innovative resolution-enhanced KMD plots [22–25]. Dividing the repeating unit by a varying integer has been accidentally found to be a satisfactory way to correct the isotopic misalignments in the present case, constituting another promising application of the fractional base units. Instead of a condition depending on the charge state only for R as the base unit (Eq. (14)), using R/X would indeed make this condition a function of the charge state *and* X.

Correction of the Isotopic Misalignments Using a Fractional Base Unit

Using a fractional base unit defined as $\frac{R}{X}$ with X an integer ≥ 1, KMs are now calculated using Eq. (4). Two consecutive oligomers at charge state z are spaced by R/z and $\Delta KM_{n-mer,\,(n+1)-mer}(R,z)$ is consequently calculated as:

$$\begin{aligned}\Delta KM_{n-mer,(n+1)-mer}(R,X,z) &= \frac{round(R/X)}{R/X}\cdot\left(m_{n-mer}/z - m_{(n+1)-mer}/z\right)\\ &= \frac{round(R/X)}{R/X}\cdot\frac{R}{z} = \frac{X\cdot round(R/X)}{z}\end{aligned} \quad (15)$$

Relying on the previous developments of equations, a *necessary and sufficient condition* for the isotopes to be properly aligned in the KMD plot is:

$$\Delta KM_{n-mer,(n+1)-mer}(R,X,z) = \frac{X\cdot round(R/X)}{z} = \text{integer} \quad (16)$$

From Eq. (16), it becomes obvious that using $X=z$ will ensure a proper alignment of points as the condition becomes:

$$\Delta KM_{n-mer,(n+1)-mer}(z) = round(R,X=z,z) = round(R/z) = \text{integer} \quad (17)$$

which is true by definition of the function "round()." The KMD plots of simulated PEO distributions computed with fractional

Table 2. Example of divisibility and indivisibility of the rounded mass of EO by the charge states accounting for the isotopic misalignment in the KMD plot (Figure 1 and Figure S1)

R	$\frac{round(R)}{z}$					
(Exact): 44.0262	$z=1$	$z=2$	$z=3$	$z=4$	$z=5$	$z=6$
(Rounded): 44	44	22	14.7	11	8.80	7.33

base units are depicted in Fig. S2. Fig. S2A displays the KMD plot indifferently calculated with EO/4, EO/2, and EO (X = 1) with a successfully realigned ion series at charge state $z = +4$. The other ion series (3+, 5+, and 6+) are nevertheless still misaligned. Using EO/3 as base unit for the computation of KMDs realigns the ion series at charge state 3+ as expected but also 5+ as the criterion $\frac{3\ \mathrm{round}(\mathrm{EO}/3)}{5}$ is an integer (Fig. S2B, same results using EO/5 correcting the 5+ and 3+ series as $\frac{5\ \mathrm{round}(\mathrm{EO}/5)}{3}$ is an integer). Eventually, X = 6 allows the ion series at charge states $z = 6+$ to be correctly aligned horizontally together with the 3+ ion series as a beneficial side effect (Fig. S2C) but does not correct the isotopic misalignment of the 4+ and 5+ series. Using the charge state as the divisor for the fractional base unit thus effectively corrects the isotopic misalignment but the realignment is done charge state by charge state except in some favorable cases.

Going one step further, using the least common multiple (LCM) of all the charge states would correct the isotopic misalignment of all the charge states at once. It is illustrated in Fig. S2D using X = 60 as divisor which is the LCM of the set of integers {3,4,5,6} realigning all the ion series horizontally regardless of the charge state. It has been proposed that the best interval for the divisor X is confined between $\mathrm{round}\left(\frac{2}{3}\mathrm{R}\right)$ and round(2R) with a preferable value of X close to round(R) [23]. This interval is based on the founding condition round(R/X) = 1 which offers the finest control over the gain of resolution. In the present case, X = 60 satisfies round(R/X) = 1 and Eq. (16) simplifies into a *sufficient* (but not necessary) condition:

$$\frac{\mathrm{X}}{z} = \text{integer} \tag{18}$$

which is obviously satisfied with the LCM of all the charge states. Such divisor also removes all the overlaps of isotopologues as exemplified with the 3+ ion series in Fig. S2D further improving the quality of ion selection in case of filtering with isotopically resolved plots.

Beyond the simulation, the KMD plot from the paper spray mass spectrum of PEO 3400 (Figure 1a) computed with the regular EO is depicted in Figure 2a displaying both the isotopic split and misalignment for the sake of reminder. In a first attempt to realign points based on the first condition defined by Eq. (16) and using the recommended values for the divisor X, a resolution-enhanced KMD plot computed with EO/48 is depicted in Figure 2b. Using X = 48 effectively realign points of same isotopic composition at charge states $z = 3$ and $z = 6$ but fails at realigning points for the $z = +5$ ion series as 48 is not divisible by 5 (inset in Figure 2b). X = 48 satisfies with the founding condition round (R/X) = 1 for a correct resolution-enhanced KMD analysis but it is not the LCM of the whole charge distribution $z = 1$–6. The actual LCM of the charge distribution is 60 and the associated resolution-enhanced KMD plot computed with the fractional base unit EO/60 is depicted in Figure 2c. Such a base unit slightly expands the KMD dimension [22] and the KMD plot is now isotopically resolved. Most importantly, the criterion defined by Eq. (18) is satisfied and the isotopes of all the charge states are correctly aligned along the *x*-axis (green dots) depending on their composition. Extracting a part of the 4+ and 3+ ion series from the KMD plot (blue solid and dotted squares, respectively) leads to the filtered mass spectra depicted in Figure 2d (4+) and Figure 2e (3+). Only one series of peaks is recovered in each case (one isotopic composition only, no interferences) and peaks are now regularly spaced by ~ 11.01 and ~ 14.68 which corresponds to the expected mass difference between consecutive PEO homologs at charge states 4+ and 3+.

This last KMD plot is the only one satisfying the founding postulate of the KMD analysis for polymer analysis claiming that species of identical elemental composition modulo R possess the same KMD value. As an interesting additional feature of the fractional base units, it is noteworthy that the interferences between charge states are also removed. With EO as the base unit, all charge states produce a line at KMD~0 with a subsequent overlap of some isotopes (Figure 2a). There is no more overlapping of the charge states when using EO/60 as all the isotopes of all the distributions line up horizontally at different KMD values (Figure 2c).

For an exhaustive exploration of the features of the KMD analysis and allied tools for multiply charged polymer ions, another application of the fractional base units for the "KMD – remainders of NKM plot" is thoroughly described in the Supporting Information. Sato et al. have introduced the notion of "remainder of NKM" (RNKM [34]) to simplify the KMD plots to the fullest [11]. The RNKM consists in the residual nominal mass once the maximum number of nominal mass of the repeating unit R (=round(R)) has been subtracted to the observed NKM of a given oligomer. For a homopolymer, RNKM is the NKM of the sum of the end groups and the adducted ion. All the congener ions of a given distribution (same end groups, same adducted ion) have identical RNKM and KMD, positioned as a single point in a so-called KMD-RNKM plot (KMD vs. RNKM) instead of a line in the KMD plot. It constitutes a powerful tool for the profiling of end groups for homopolymers [11] and for evaluating the discrete co-monomeric composition of copolymers [34]. However, multiple charging has been found to induce another "split of the remainders" in addition to the isotopic split in the KMD dimension which dramatically complicates the visualization of data in the KMD-RNKM plots (charge state *z*: *z* lines in the KMD plot and *z* values of $\mathrm{RNKM} = z^2$ groups of points in the KMD-RNKM plot instead of one; Fig. S3). The use of fractional base units with the charge state or the LCM of the charge states as divisors proposed above to overcome the isotopic misalignment also successfully removes the split of RNKMs (Fig. S4-S6). Such correction is nevertheless not free of side effects and might limit the use of the KMD-RNKM analysis to simple samples in case of multiple charging.

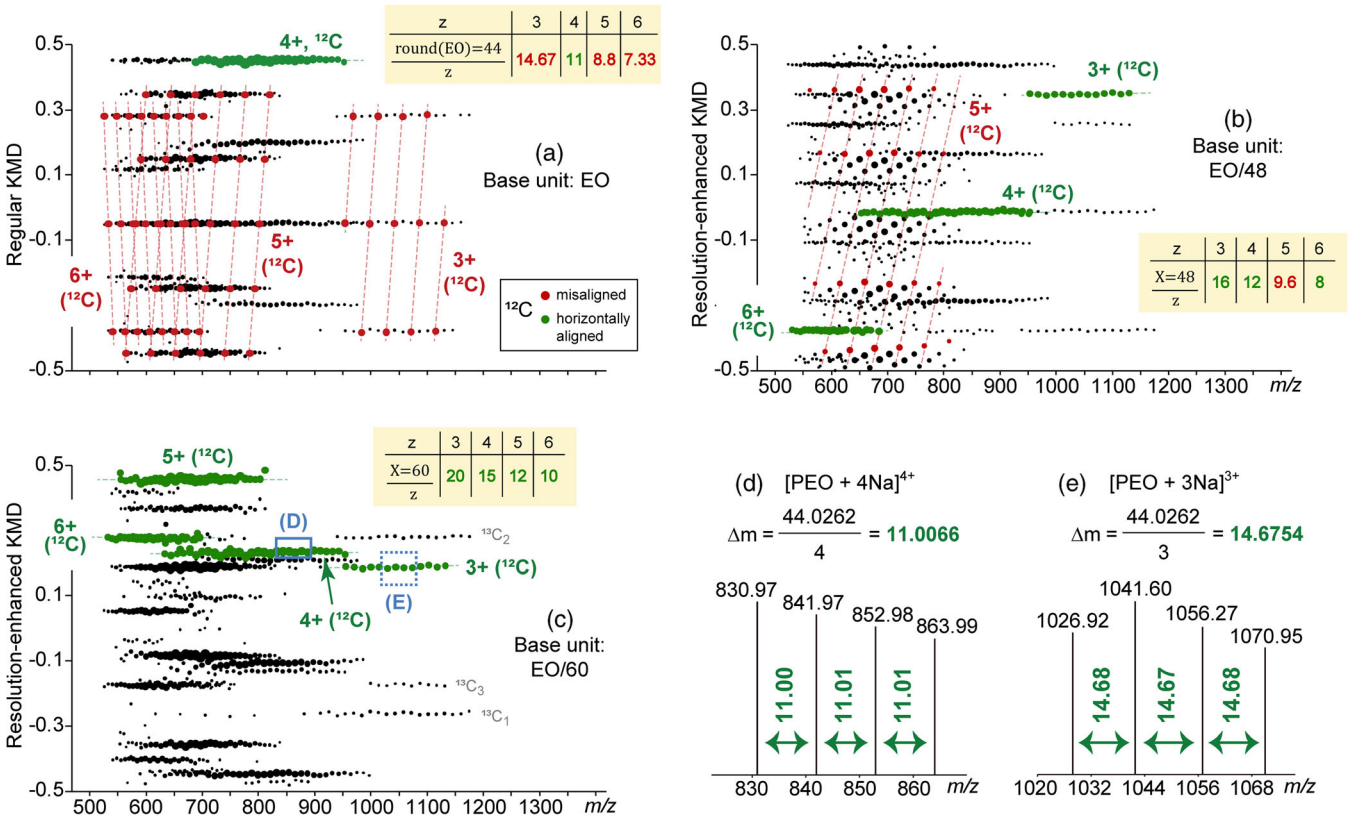

Figure 2. KMD plot from the paper spray mass spectrum of PEO 3400 using (**a**) EO, (**b**) EO/48, and (**c**) EO/60 as the base units. Divisibility/indivisibility of the divisor by the charge states are listed in yellow insets. (**d**, **e**) Mass spectra from the 4+ and 3+ ion series extracted from the KMD plot

Removing the Isotopic Split Using the Charge-Dependent KMDs and the Remainders of Kendrick Mass

The isotopic split of multiply charged ion series is informative since the charge state distribution can be evaluated at first sight in the regular KMD plot. However, and despite the realignment of isotopes using the fractional base units, such split is also detrimental to an easy data processing. Several lines should be selected to get a full distribution with the risk of strong interferences for complex samples. It might thus be of interest to remove the isotopic split in some situations to facilitate the grouping of series via one single selection. The isotopic split and misalignment arise from the term "$1/z$" found in the computation of KMDs (Eq. (10)), itself arising from the term "m/z" in the definition of KMs (Eq. (2)). An intuitive way to cluster a split ion series at charge state z thus simply consists of multiplying all the KMs by z to remove the contribution of this charge state in KMs and KMDs while the other charge states are left untouched. The notion of regular "charge-dependent KM" noted KM(R,Z) is introduced here for the first time:

$$\mathrm{KM(R,Z)} = \mathrm{Z}\cdot\mathrm{KM(R)} = \mathrm{Z}\cdot m/z \cdot {}^{\mathrm{round(R)}}/_{\mathrm{R}} \qquad (19)$$

with "Z" being a charge state chosen by the user as input while "z" designates the actual charge state of the ion at a given m/z.

The regular KMD plot from the paper spray mass spectrum of PEO 3400 is depicted in Figure 3a as the reference plot. A new regular charge-dependent KMD plot computed with Z = 3 (i.e., multiplying all the KMDs of the regular KMD plot by 3) is depicted in Figure 3b and displays the expected clustering of the 3+ ion series into a single group of points while the ion series at charge states 4+ and 5+ are still split in four and five lines, respectively. As a spin off, the ion series at charge state 6+ is now split in two lines in lieu of six in the regular KMD plot via a partial removal of the isotopic split. The charge-dependent KMD plots with Z = 4 (Figure 3c) and Z = 5 (Figure 3d) display the ion series at charge states 4+ and 5+ clustered in a single cloud one by one. It is a reminiscence of the previous situation using the fractional base units to correct the isotopic misalignment using a multiplier instead of a divisor. However and in spite of a successful removal of the split, plots become more and more fuzzy with a clear degradation of the quality of point alignments. Multiplying KMDs by an integer also induces the errors in mass measurements (i.e., variations of KMDs and slight deviation from the horizontal alignments) to be multiplied as well.

Such degradation of the quality of point alignment as observed with low-resolution or high-mass datasets has been previously overcome by using the fractional base

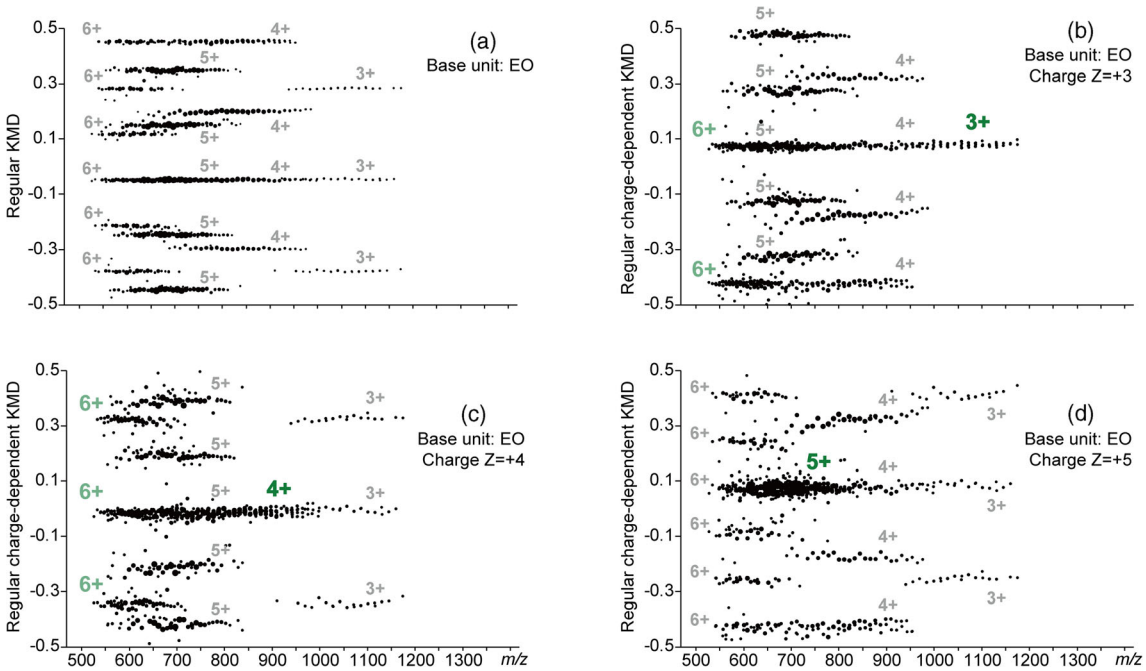

Figure 3. (**a**) Regular KMD plot from the paper spray mass spectrum of PEO 3400 (base unit: EO). Regular charge-dependent KMD plots using (**b**) Z = +3, (**c**) Z = +4, and (**d**) Z = +5

units to plot the so-called resolution-enhanced KMD plots [25]. The definition of the charge-dependent KMs does not prevent from using a fractional base unit:

$$\mathrm{KM}(\mathrm{R},\mathrm{Z},\mathrm{X}) = \mathrm{Z}\cdot\mathrm{KM}(\mathrm{R},\mathrm{X}) = \mathrm{Z}\cdot m/z\cdot{}^{\mathrm{round}(\mathrm{R}/\mathrm{X})}/_{\mathrm{R}/\mathrm{X}} \qquad (20)$$

Contrary to the previous case about the realignment of isotopes, there is no limitation in terms of divisors. Since the charge state Z to be clustered is no longer considered in the calculation of KM(D)s, the divisor does not longer need to be divisible by the charge state and any divisor ranging from round(2/3R) to round(2R) [23] can be chosen depending on the gain of resolution needed. The versatility of the resolution-enhanced KMD plots is thus fully restored as shown with the charge-dependent *and* resolution-enhanced KMD plots computed from the paper spray mass spectrum of PEO 3400 using EO/42 and Z = +3 to cluster the 3+ ion series (Figure 4b), EO/42 and Z = +4 (Figure 4c), or EO/41 and Z = +5 (Figure 4d) to cluster the 4+ and 5+ ion series, respectively. With the gain of separating power resulting from the use of a fractional base unit, the clustered ion series is now displayed as an isotopically resolved single cloud with several horizontal lines assigned to the ^{12}C and $^{13}C_x$ isotopes (Figure 4b–d) to be compared to the initial and multi-biased regular KMD plot computed with EO (Figure 4a, equivalent to a regular charge-dependent KMD with Z = 1) displaying both the isotopic split and misalignment.

A certain misalignment of points remains despite a gain of resolution higher than usual (default divisor for the resolution-enhanced KMD plots of PEO polymers: X = round(EO)-1 = 43 [23] while X = 42 and X = 41 are used in Figure 4). The remainders of KMs [33] newly introduced for the data processing of low resolution TOF/TOF data and oligomerically resolved mass spectra have been specifically designed to overcome this limitation. The original RKMs are computed using the following equation:

$$\mathrm{RKM}(\mathrm{R}) = \left\{\frac{\mathrm{KM}(\mathrm{R})}{\mathrm{round}(\mathrm{R})}\right\} = \left\{m/z\cdot\frac{{}^{\mathrm{round}(\mathrm{R})}/_{\mathrm{R}}}{\mathrm{round}(\mathrm{R})}\right\} = \left\{\frac{m/z}{\mathrm{R}}\right\} \qquad (21)$$

with {} being the fractional part function defined as {x} = x − floor(x). It simply consists of dividing *m/z* by the exact mass of the repeating unit and keeping its fractional part. At first sight, it becomes obvious that computing a new "charge-dependent" RKM using round(R)/Z instead of round(R) would remove the chosen charge state Z from the equation as follows:

$$\mathrm{RKM}(\mathrm{R},\mathrm{Z}) = \left\{\frac{\mathrm{KM}(\mathrm{R})}{{}^{\mathrm{round}(\mathrm{R})}/_{\mathrm{Z}}}\right\} = \left\{\frac{m/z\cdot{}^{\mathrm{round}(\mathrm{R})}/_{\mathrm{R}}}{{}^{\mathrm{round}(\mathrm{R})}/_{\mathrm{Z}}}\right\} = \left\{\frac{\mathrm{Z}\cdot m/z}{\mathrm{R}}\right\} \qquad (22)$$

which simplifies in $\left\{\frac{\mathrm{m}}{\mathrm{R}}\right\}$ if the charge state of the ion is equal to the chosen input Z (Z = *z*). Being now free of the charge, there is neither an isotopic split nor any isotopic misalignment and the so-obtained charge-dependent RKM plot would display a clustered ion series at charge state Z with homologous polymer ions being aligned horizontally. As a first step, the KMD plot computed from the actual paper spray mass spectrum of PEO 3400 used as the reference plot throughout the article

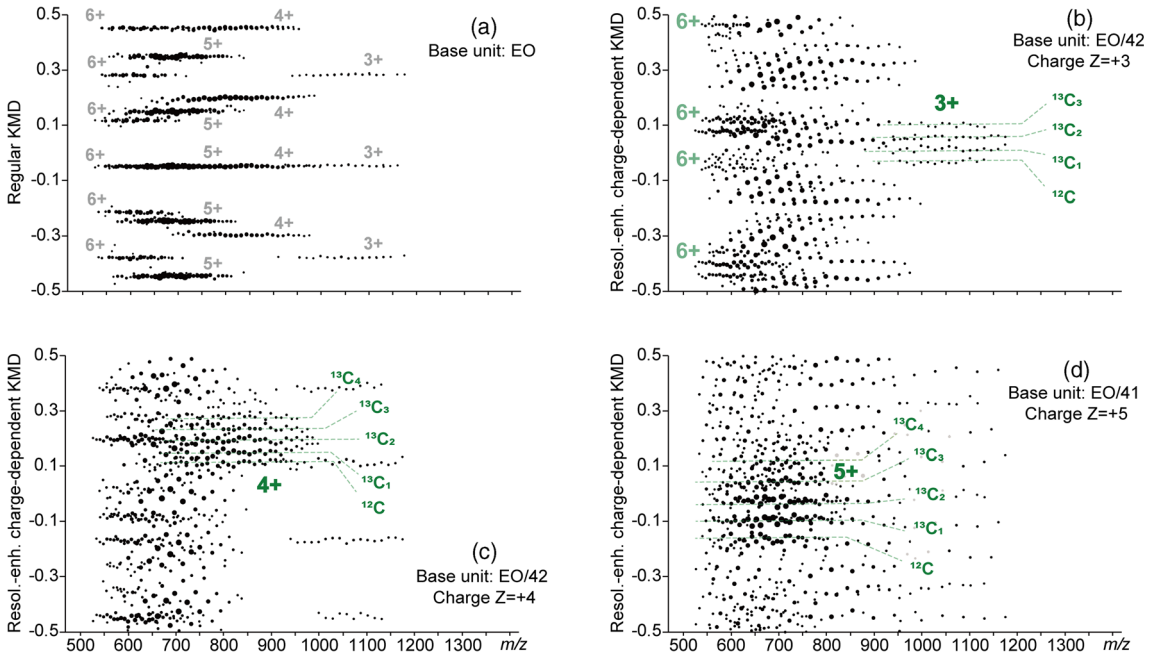

Figure 4. (**a**) Regular KMD plot from the paper spray mass spectrum of PEO 3400 (base unit: EO). Resolution-enhanced charge-dependent KMD plots using (**b**) EO/42 and Z = +3, (**c**) EO/42 and Z = +4, and (**d**) EO/41 and Z = +5

(Figure 5a) is turned into a regular RKM plot computed with EO and round(EO) (i.e., Z = 1; Figure 5b). Slight misalignments of points arising from inaccuracies in the mass measurements are corrected [33] and ion series are displayed at straight horizontal lines while the isotopic split is still observed. Second, a new charge-dependent RKM plot using Z = +3 (i.e., dividing KMs by round(EO)/3) to cluster the 3+ series) is depicted in Figure 5c. A single cloud of point is observed in lieu of the three main lines which allows the full distribution to be recovered in one single selection (green shape and inset in Figure 5c, black lines for the 3+ ion series over the full mass spectrum in gray). Similar results are obtained for the 4+, 5+, and 6+ ion series using the charge-dependent RKMs computed with Z = +4 to +6 and displaying the expected clustered ion series in each case (Figure 5d–f). Such a clear grouping of points allows a neat selection of the whole distribution in the mass spectrum (insets in Figure 5c–f) which would not be possible using the regular KMD plots owing to the overlapping of points at KMD~0 common to all the charge states (Fig. S7). As a major spin off, clustering ion series also facilitates the assignment of points as exemplified by three unexpected series clearly popping up in the RKM plot using Z = +5 (Figure 5e) and Z = +6 (Figure 5f) assigned to $[M + 3Na + Ca]^{5+}$, $[M + 2Na + H + Ca]^{5+}$ and $[M + 4Na + Ca]^{6+}$ calcium adducts. These minor series were not isolated neither in the original mass spectrum owing to their low intensity nor in the regular KMD plot (Figure 5a) owing to the limited quality of point alignment, the high number of points, and the isotopic split.

Combining the Regular KMDs, Resolution-Enhanced KMDs, and RKMs in a Single Equation to Generate the Associated Plots with a Unique Set of Inputs

At this point, a user may thus choose to compute a regular or a regular charge-dependent KMD plot, a resolution-enhanced or a resolution-enhanced charge-dependent KMD plot, or a charge-dependent RKM plot to visualize the charge state distribution, realign isotopes, or select ion series easily. However, several input parameters have been introduced throughout the text such as the repeating unit R, a divisor X = round(R) + n, and a charge Z. Every plot is seemingly computed with its own set of parameters making the data processing apparently complex. By expanding the definition of the resolution-enhanced charge-dependent KMs (Eq. (20), noted KM(R,Z,X)), it is demonstrated that the three main outputs (regular KM, resolution-enhanced KM, and RKM) are linked in a single equation in spite of their sequential introduction in the literature which means their inputs are also linked. Starting from round(R), the recommended divisor X is calculated as X = round(R) + n with n being an integer (positive or negative) [23]. The default value is typically X = round(R)-1 (e.g., X = 43 for PEO, n = − 1) and iteratively decreased (e.g., n = − 2, − 3, − 4…) or increased (e.g., n = +1, +2, +3…) until a satisfactory separation of ion series is reached (Figure 4). The resolution-enhanced charge-dependent KMs may thus be written as a function of n instead of X as follows:

$$\mathrm{KM}(\mathrm{R},\mathrm{Z},\mathrm{n}) = \mathrm{Z}\cdot m/z\cdot \frac{\mathrm{round}\left({}^{\mathrm{R}}/_{(\mathrm{round}(\mathrm{R})+\mathrm{n})}\right)}{{}^{\mathrm{R}}/_{(\mathrm{round}(\mathrm{R})+\mathrm{n})}} \qquad (23)$$

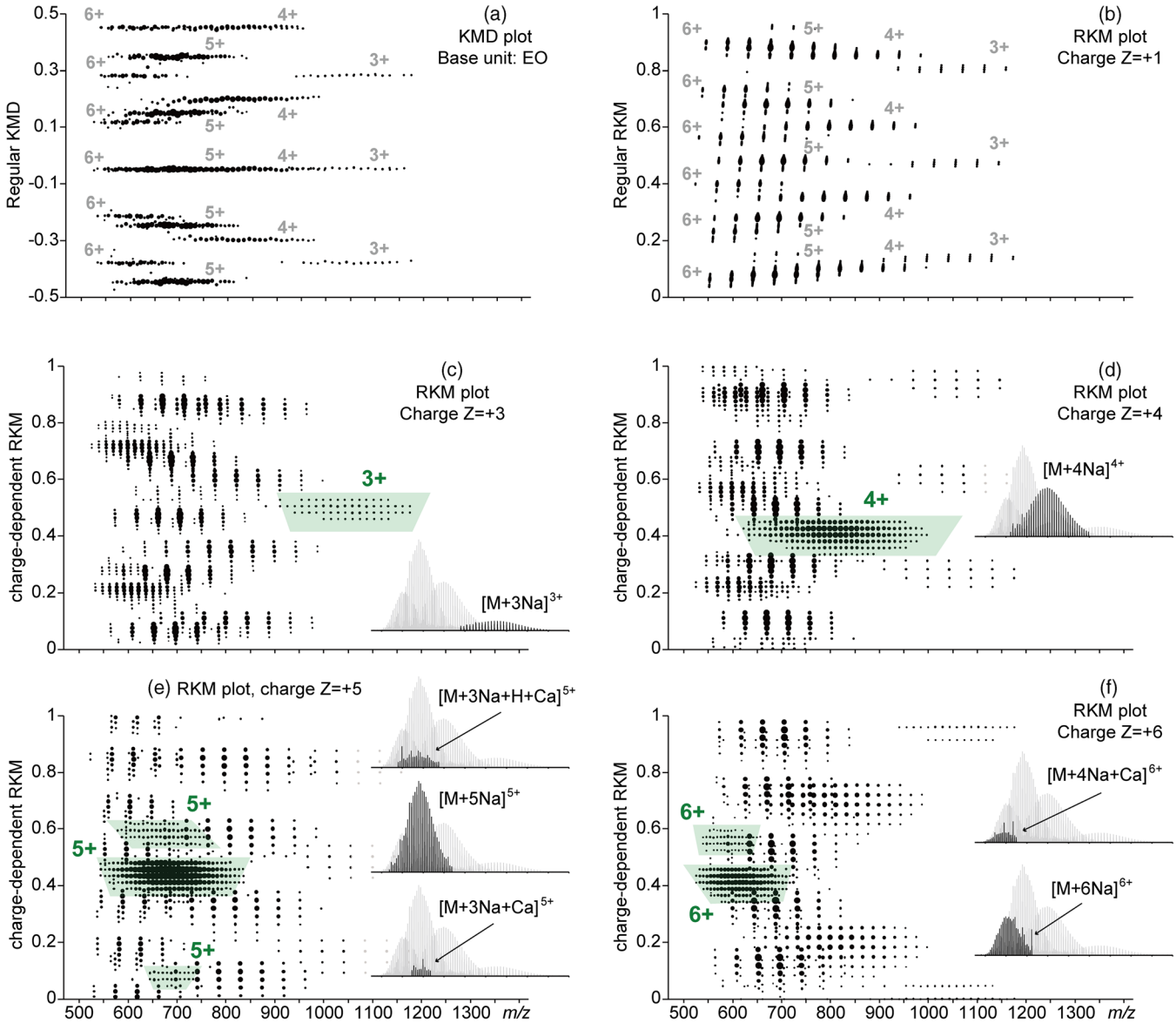

Figure 5. (**a**) Regular KMD plot from the paper spray mass spectrum of PEO 3400 (base unit: EO). (**b**) Regular RKM plot (EO, Z = +1). Charge-dependent RKM plots using (**c**) Z = +3, (**d**) Z = +4, (**e**) Z = +5, and (**f**) Z = +6. Insets: filtered mass spectra of the clustered ion series extracted from the RKM plots (green shape and black line) and full mass spectrum (gray line)

Of note, this definition contains all the latest refinements [11, 22, 23] to be compared to the historical definition of a Kendrick mass ($KM = m/z \cdot {}^{14}/_{14.0157}$; Eq. (1)) for a better emphasis on the recent evolution of this data processing tool. The choice of a divisor X = round(R) + n is based on the founding principle round(R/X) = 1 [23] and Eq. (23) becomes:

$$\mathrm{KM(R,Z,n)} = \mathrm{Z}\cdot m/z\cdot\frac{\mathrm{round(R)}+\mathrm{n}}{\mathrm{R}} = \mathrm{Z}\cdot m/z\cdot\frac{\mathrm{round(R)}}{\mathrm{R}} + m/z\cdot\frac{\mathrm{Z}\cdot\mathrm{n}}{\mathrm{R}} \tag{24}$$

The first term $\mathrm{Z}\cdot m/z\cdot\frac{\mathrm{round(R)}}{\mathrm{R}}$ is simply KM(R, Z) (Eqs. (2) and (19)), i.e., the regular charge-dependent KM with no fractional base unit. The second term $m/z\cdot\frac{\mathrm{Z}\cdot\mathrm{n}}{\mathrm{R}}$ is the first part of RKM(R, Z*n) using ${}^{\mathrm{round(R)}}/_{\mathrm{Z}}\cdot\mathrm{n}$ instead of round(R) as divisor. Switching to the KMD/RKM dimension is readily done by adding/subtracting round(KM(R,Z)), round(KM(R,Z,n)), and floor() to both parts of Eq. (24) as follows:

$$\begin{aligned}&\mathrm{KM(R,Z,n)}-\mathrm{round(KM(R,Z,n))}-\mathrm{KM(R,Z)}\\&\quad+\mathrm{round(KM(R,Z))}-\mathrm{floor}\left(m/z\cdot\frac{\mathrm{Z*n}}{\mathrm{R}}\right)\\&=m/z\cdot\frac{\mathrm{Z*n}}{\mathrm{R}}-\mathrm{floor}\left(m/z\cdot\frac{\mathrm{Z*n}}{\mathrm{R}}\right)-\mathrm{round(KM(R,Z,n))}\\&\quad+\mathrm{round(KM(R,Z))}\end{aligned} \tag{25}$$

By the definition of KMs and RKMs, the term $\mathrm{round}(\mathrm{KM}(\mathrm{R},\mathrm{Z},\mathrm{n}))+\mathrm{round}(\mathrm{KM}(\mathrm{R},\mathrm{Z}))-\mathrm{floor}\left(m/z\cdot\frac{\mathrm{Z*n}}{\mathrm{R}}\right)$ is an integer equal to 0 or 1 whatever R and n at charge state $z=+1$ and becomes 0, 1, 2,… up to z at charge state z owing to the round/floor functions. The integer part does not impact on the KMD/RKM dimension so Eq. (25) is readily simplified into

$$\mathrm{KMD}(\mathrm{R},\mathrm{Z})-\mathrm{KMD}(\mathrm{R},\mathrm{Z},\mathrm{n})=\mathrm{RKM}(\mathrm{R},\mathrm{Z*n}) \quad (26)$$

Subtracting a resolution-enhanced charge-dependent KMD plot computed with ${}^{\mathrm{R}}/_{\mathrm{round(R)+n}}$ as base unit and Z as charge state to its regular charge-dependent counterpart computed with R as base unit and Z as charge state thus gives a related resolution-enhanced charge-dependent RKM plot computed with an *apparent* charge state Z*n.

Such a relationship is graphically revealed in Figure 6 with the resolution-enhanced charge-dependent KMD plot from the paper spray mass spectrum of PEO 3400 using EO/42 as base unit (X = round(EO) + n = 44 + (− 2) = 42, n = − 2) and Z = +3 to cluster the 3+ ion series (Figure 6b; one group for 3+ with isotopic resolution, four groups for 6+) subtracted to the regular charge-dependent KMD plot (base unit: EO, charge Z = +3; Figure 6c; one line for 3+ and two lines for 6+). The resulting plot is a resolution-enhanced charge-dependent RKM computed with EO as base unit and an apparent charge Z*n = +3*(− 2) = − 6 (i.e., dividing KMs by -round(EO)/6; Figure 6c). The RKM plot displays three clustered groups of points isotopically resolved for the 3+ ion series ($[\mathrm{M}+3\mathrm{Na}]^{+}$) and the two 6+ ion series ($[\mathrm{M}+6\mathrm{Na}]^{+}$ and $[\mathrm{M}+4\mathrm{Na}+\mathrm{Ca}]^{+}$). In a nutshell, the errors of mass measurements leading to slight misalignments of points in the regular and resolution-enhanced KMD plots are canceled by their subtraction while the resulting RKM plot exhibits the same separation capabilities as the resolution-enhanced KMD plot. It is also confirmed with the resolution-enhanced charge-dependent KMD plot computed with EO/46 and Z = +4 (n = +2; Figure 6d) subtracted to the regular charge-dependent KMD plot (EO, Z = +4; Figure 6e) producing a resolution-enhanced charge-dependent RKM plot computed with an apparent charge Z*n = + 8 (Figure 6f). The simple development of a rigorous mathematical background thus provides a unified theory with the three plots composing the so-called advanced KMD analysis being eventually linked to each other. A unique set of inputs—a repeating unit R easily chosen depending on the polymer to be analyzed, a charge Z to be clustered, and a divisor X or an integer n (the only parameter a user may modify depending on the required resolution)—are sufficient to simultaneously compute all the plots presented in the article.

Beyond a Single-Stage MS and Homopolymers: Extension to MS/MS Data of PEO and MS Data of P(EO-b-PO-b-EO)

Each plot composing the "advanced KMD analysis" brings some pieces of information depending on the user's need while their computation is done in a single step. It is illustrated with two examples of data processing for the ESI-CAD mass spectrum of multiply charged PEO oligomers (regular and resolution-enhanced KMD plots) and the paper spray mass spectrum of a EO/PO triblock copolymer (resolution-enhanced KMD and RKM plots).

A set of multiply charged PEO oligomers from the ESI-MS of PEO 6000 have been isolated (selected range: m/z 972–1015) and activated via collision at low energy to reduce their charge states and simplify the interpretation of data (Figure 7a). Selected oligomers are mainly 6+ but several other charge states are clearly observed in the CAD mass spectrum when zooming on the precursor ions (inset in Figure 7a). Product ions are detected in a higher mass range as compared to the precursor ions since their charge state is decreasing. Instead of manually evaluating the charge state distribution of both the precursor and product ions by assigning each peak one by one, a rapid analysis is achieved by plotting the regular KMD plot from the MS/MS data using EO as the base unit (Figure 7b). Advantageously relying on the isotopic split, the charge state distribution is instantly visualized by counting lines in the KMD plot (Figure 7b, green shapes) with product ions at charge states ranging from 2+ (two lines) to 6+ (six lines). As suspected from the ESI-CAD mass spectrum itself and confirmed by the regular KMD plot displaying numerous lines, the charge state distribution of the precursor ions is not that simple and requires additional plots.

The regular charge-dependent KMD plots focused on the precursor ions computed with EO and Z = 3–7 are depicted in Figure 7c displaying one main clustered line associated with the precursor ions at the chosen charge state. Plots remain nevertheless fuzzy owing to the great number of points or even fail at separating the precursor ions at charge states 3+ and 6+ (Figure 7c, left plot). The visualization of data is greatly improved by plotting the resolution-enhanced charge-dependent KMD plots using EO/43 (default divisor X = 43) and Z = 3–7 (Figure 7d). Each series of precursor ions at the chosen charge state is now clustered in a single cloud and clearly separated from all the other disordered points. Each cloud is isotopically resolved and the number of oligomers at the chosen charge state in the selected mass range for MS/MS is readily deduced as well (e.g., four 4+ and 5+ congeners, five 6+ congeners). The uncertainty about the charge states 3+ and 6+ is also favorably removed using Z = 3 (Figure 7d, left plot) with the two minor 3+ oligomers isolated from the five main 6+ precursor ions split in two groups. The charge state distribution of both the precursor ions and the product ions is thus deciphered within a minute with a single-step data processing using the regular KMD plot (isotopic split) and the resolution-enhanced charge-dependent KMD plot (clustering and separation) computed simultaneously.

The charge states proposed above do not exceed +7 as a typical upper limit for the charge state distribution of multiply charged polymer ions observed in a ESI mass spectrum. However, the methodology would be fully compatible with higher charge states in the case of particularly high molecular weight

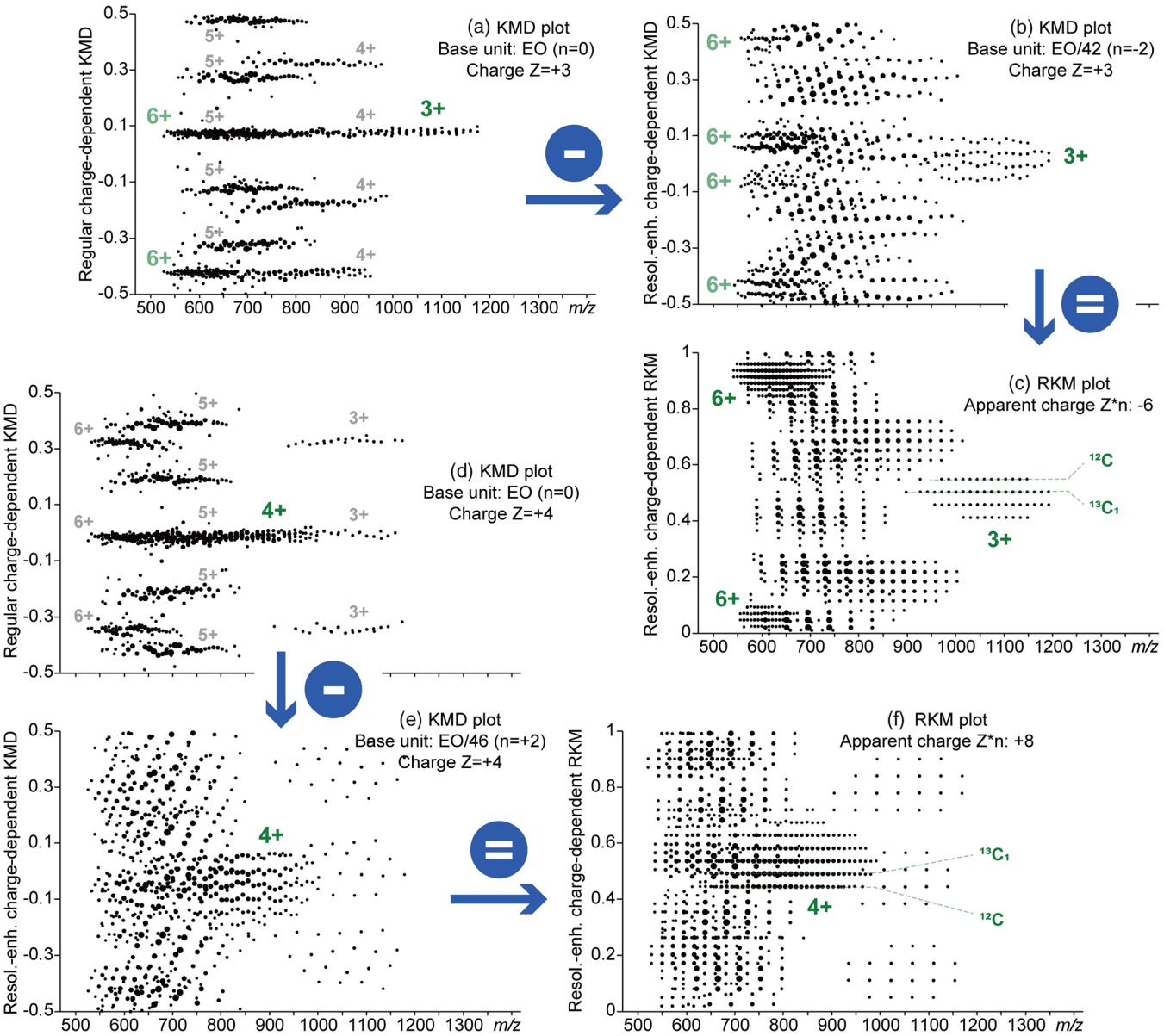

Figure 6. (**a**) Regular charge-dependent KMD plot from the paper spray mass spectrum of PEO 3400 (EO, Z = +3). (**b**) Resolution-enhanced charge-dependent KMD plot (EO/42, n = – 2 and Z = +3). (C) Resolution-enhanced charge-dependent RKM plot (apparent charge Z*n = + 6) strictly equivalent to the difference of the first two plots. (**d**) Regular charge-dependent KMD plot (EO, Z = + 4). (**e**) Resolution-enhanced charge-dependent KMD plot (EO/46, n = + 2 and Z = + 4). (**f**) Resolution-enhanced charge-dependent RKM plot (apparent charge Z*n = + 8) strictly equivalent to the difference of the first two plots

samples or with a particularly high propensity for multiple charging. A hypothetic upper limit for the charge state observable in a regular KMD plot via the isotopic split (z lines at charge state z) can be speculated first considering $\Delta\mathrm{KMD}_{^{13}\mathrm{C}_1,^{12}\mathrm{C}}(\mathrm{R}=\mathrm{EO}, z=1)\sim -0.0028$ and an arbitrary minimal separation of the z lines set at $\Delta\mathrm{KMD}_{^{13}\mathrm{C}_1,^{12}\mathrm{C}}(\mathrm{R}=\mathrm{EO}, z) > 10\cdot\Delta\mathrm{KMD}_{^{13}\mathrm{C}_1,^{12}\mathrm{C}}(\mathrm{R}=\mathrm{EO}, z=1)\sim -0.0280$ to avoid any overlapping. Finally considering the spectral width of a KMD plot at $\Delta\mathrm{KMD} = 0.5-(-0.5) = 1$, the highest charge state identifiable in the KMD plot—i.e., the maximal number of lines readily distinguishable—would be $z_{\max}(\mathrm{R}=\mathrm{EO}) = {}^{1}/_{\Delta\mathrm{KMD}_{^{13}\mathrm{C}_1,^{12}\mathrm{C}}(\mathrm{R}=\mathrm{EO},z)} \sim 36$. More prosaically, the capabilities of the mass analyzer to separate the isotopes of an isotopic distribution at charge state z is the main limiting factor. In other words, the main limitation comes from the MS step itself (instrument and user), not from the data processing step. About the charge-dependent and/or resolution-enhanced KMD or RKM plots, the versatility of the methodology is high enough to virtually process ion series at any charge state directly thanks to the wide range of divisors available and thanks to the removal of the isotopic split itself by means of the charge-dependent computation canceling the "z" term in the equations.

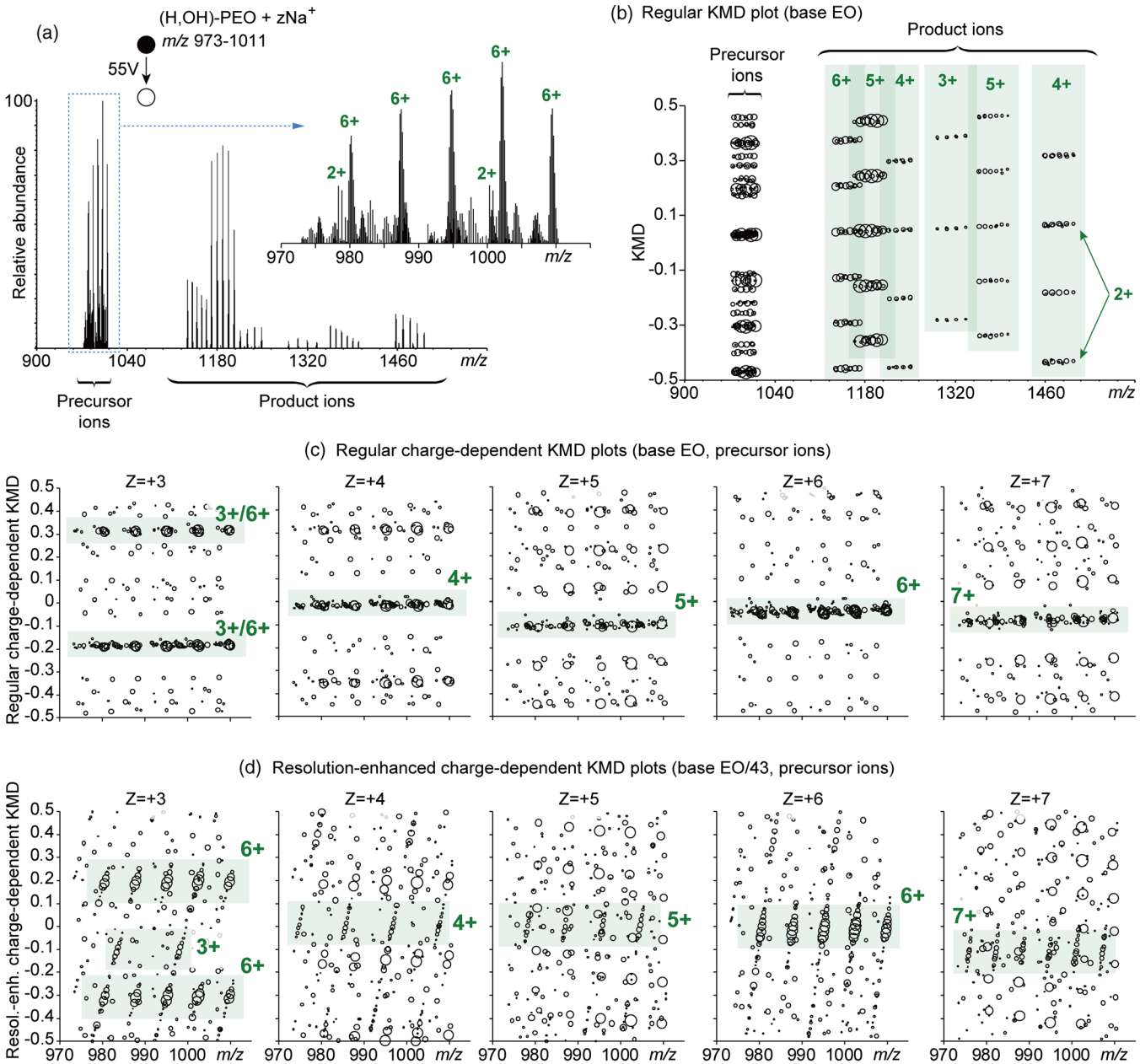

Figure 7. (**a**) ESI-CAD mass spectrum of a set of multiply charged PEO oligomers for charge reduction purposes. Inset: zoom on the precursor ions. (**b**) Regular KMD plot (base unit: EO, whole spectrum). (**c**) Regular charge-dependent KMD plots (EO, Z = +3–+7) and (**d**) resolution-enhanced charge-dependent KMD plots (EO/43, Z = +3–+7) from the precursor ions only

Eventually, a triblock P(EO-*b*-PO-*b*-EO) copolymer has also been mass analyzed by paper spray MS to check at the validity of the KMD analysis of multiply charged *copolymer* ions. The KMD plots computed from homopolymers display lines as a unique repeating unit is present while KMD plots of copolymers are typically elliptic at charge state 1+ due to the contribution of (at least) two repeating units (horizontal alignment of co-oligomers differing by their content in one co-monomer used as base unit for KMDs and oblique alignment for any variation of the content in the other co-monomer or end groups). A similar situation has been reported for multiply charged copolymer ions with several elliptic clouds of points due to the isotopic split [31].

It is illustrated with the regular KMD plot computed from the paper spray mass spectrum of P(EO-*b*-PO-*b*-EO) 2000 using EO as base unit depicted in Figure 8a (Fig. S8 in the Supporting Information for the alternative KMD analysis using PO as base unit). Six groups of points are observed assigned to the co-oligomers at charge state 1+ (one group), 2+ (two groups), and 3+ (three groups). Two horizontal lines are seen in the low mass range and assigned to singly charged PEO product ions formed upon in-source decay (ISD) which validate a block architecture. The regular charge-dependent KMD

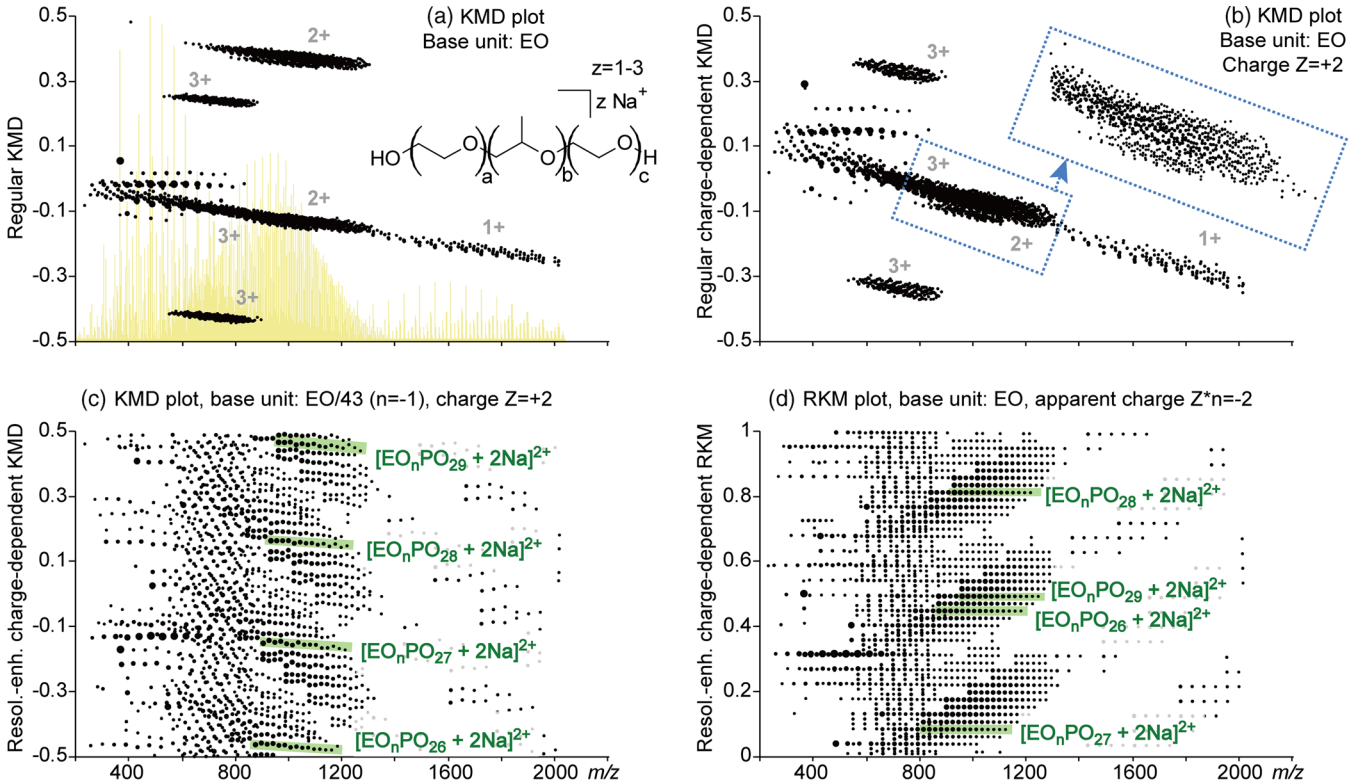

Figure 8. (**a**) Regular KMD plot from the paper spray mass spectrum of P(EO-*b*-PO-*b*-EO) (background plot, yellow line) using EO as base unit. (**b**) Regular charge-dependent KMD plot (EO, Z = +2). Inset: zoom on the clustered 2+ series. (**c**) Resolution-enhanced charge-dependent KMD plot (EO/43, Z = +2). (**d**) Resolution-enhanced charge-dependent RKM plot (apparent charge Z*n = –2). EO_n-$PO_{26–29}$ double-sodiated co-oligomers are highlighted with green shapes

plot computed with EO and Z = +2 successfully clusters the 2+ copolymeric ion series in a single elliptic group of points as for the case of homopolymers (Figure 8b) while points cannot be assigned due to a low resolving power (fuzzy pot, inset in Figure 8b). Its resolution-enhanced counterpart using EO/43 (default divisor X = round(EO) + n = 43, n = − 1) readily separates all the co-oligomers at charge state 2+ based on their content in PO (e.g., EO_n-$PO_{26–29}$ isolated with green shapes; Figure 8c) as reported previously in case of single charging [22]. The three main groups of points are no longer due to any isotopic split but arise from the expansion of the KMD dimension with the use of a fractional base unit improving the separation of ions. Slight point misalignments arising from inaccuracies of the mass measurements are finally corrected in the associated resolution-enhanced charge-dependent RKM plot automatically computed from the inputs of the regular and resolution-enhanced KMD plots (Z*n = −2; Figure 8d) with straight horizontal lines for an even easier selection of points in grouping mode to filter a given co-oligomeric series.

This last example dealing with an additional PO repeating unit briefly tackles the applicability of this methodology regarding the type of polymeric samples. If a unique PEO reference polymer has been used throughout the text to make the discussion as didactic as possible, the regular/charge-dependent/resolution-enhanced KMD analysis is compatible with any homo/co/terpolymeric backbone regardless of the nature of the repeating unit(s) (from the simplest methylene moiety CH_2 at 14.0157 in the IUPAC scale to a large ethylene terephthalate $C_{10}H_8O_4$ at 192.0423 or even larger). If the exact mass of (at least) one monomer is known as the only initial piece of information required for a KMD analysis whatever its variation, informative alignments and clustering of ion series would be displayed in the KMD plots.

Conclusion

Meeting the need for a theoretical framework accompanying the powerful but still empirical KMD analysis of polymer ions, simple mathematics have been developed to account for (a) the origin of the isotopic split in the KMD plots of multiply charged ions, (b) the misalignment of isotopes for some charge states and repeating units, (c) the correction of this misalignment using a fractional base unit, and (d) the clustering of split isotopes using a new charge-dependent KMD and/or the RKM procedure. It constitutes a new example of the ever-widening range of applications of the fractional base units and the RKM plot in addition to the resolution-enhanced KMD analysis and the extension of mass defect analysis to low-resolution datasets. Depending on the need, a user can easily manipulate KMDs (or RKMs, same dimension) from single stage or tandem mass spectrometry of homo- and copolymers by choosing

one or the other technique for a rapid evaluation of the charge state distribution (regular KMD analysis), an unbiased extraction of data, or a better assignment of ion series (fractional base units and/or RKM plot) in a single data processing step with a unique set of parameters. In particular, the clustering of the split ion series makes the KMD analysis powerful again with the capability to distinguish distributions with different chain ends, supernumerary repeating units in blends of different homopolymers and/or co/terpolymeric series, or evaluate the comonomeric contents among other features. All are important pieces of information for the molecular characterization of industrial polymeric materials. These tools are under implementation in commercial software for a user-friendly KMD analysis of mass spectra.

Funding Information

T. Fouquet and H. Sato acknowledge the past financial support by the Japan Society for the Promotion of Science (JSPS) under the postdoctoral fellowship for overseas researchers program (FY2015) and a Grant-in-Aid "JSPS KAKENHI" (Grant Number: JP 15F15344).

References

1. Sleno, L.: The use of mass defect in modern mass spectrometry. J. Mass Spectrom. **47**, 226–236 (2012)
2. Meija, J.: Mathematical tools in analytical mass spectrometry. Anal. Bioanal. Chem. **385**, 486–499 (2006)
3. Cho, Y., Ahmed, A., Islam, A., Kim, S.: Developments in FT-ICR MS instrumentation, ionization techniques, and data interpretation methods for petroleomics. Mass Spectrom. Rev. **34**, 248–263 (2015)
4. Van Loon, A., Genuit, W., Pottasch, C., Smelt, S., Noble, P.: Analysis of old master paintings by direct temperature-resolved time-of-flight mass spectrometry: some recent developments. Microchem. J. **126**, 406–414 (2016)
5. Ubukata, M., Jobst, K.J., Reiner, E.J., Reichenbach, S.E., Tao, Q., Hang, J., Wu, Z., Dane, A.J., Cody, R.B.: Non-targeted analysis of electronics waste by comprehensive two-dimensional gas chromatography combined with high-resolution mass spectrometry: using accurate mass information and mass defect analysis to explore the data. J. Chromatogr. A. **1395**, 152–159 (2015)
6. Ortiz, X., Jobst, K.J., Reiner, E.J., Backus, S.M., Peru, K.M., McMartin, D.W., O'Sullivan, G., Taguchi, V.Y., Headley, J.V.: Characterization of naphthenic acids by gas chromatography-Fourier transform ion cyclotron resonance mass spectrometry. Anal. Chem. **86**, 7666–7673 (2014)
7. Qi, Y., Hempelmann, R., Volmer, D.A.: Two-dimensional mass defect matrix plots for mapping genealogical links in mixtures of lignin depolymerisation products. Anal. Bioanal. Chem. **408**, 4835–4843 (2016)
8. Dier, T.K.F., Egele, K., Fossog, V., Hempelmann, R., Volmer, D.A.: Enhanced mass defect filtering to simplify and classify complex mixtures of lignin degradation products. Anal. Chem. **88**, 1328–1335 (2016)
9. Vallverdú-Queralt, A., Meudec, E., Eder, M., Lamuela-Raventos, R.M., Sommerer, N., Cheynier, V.: Targeted filtering reduces the complexity of UHPLC-Orbitrap-HRMS data to decipher polyphenol polymerization. Food Chem. **227**, 255–263 (2017)
10. Vallverdú-Queralt, A., Meudec, E., Eder, M., Lamuela-Raventos, R., Sommerer, N., Cheynier, V.: The hidden face of wine polyphenol polymerization highlighted by high-resolution mass spectrometry. ChemistryOpen. **6**, 336–339 (2017)
11. Sato, H., Nakamura, S., Teramoto, K., Sato, T.: Structural characterization of polymers by MALDI spiral-TOF mass spectrometry combined with Kendrick mass defect analysis. J. Am. Soc. Mass Spectrom. **25**, 1346–1355 (2014)
12. Kendrick, E.: A mass scale based on CH2 = 14.0000 for high resolution mass spectrometry of organic compounds. Anal. Chem. **35**, 2146–2154 (1963)
13. Marshall, A.G., Rodgers, R.P.: Petroleomics: the next grand challenge for chemical analysis. Acc. Chem. Res. **37**, 53–59 (2004)
14. Heppner, R.A., Knox, J.M.: Computer-analysis of high-resolution mass-spectral data from mixtures of organic-compounds. Chem. Biomed. Environ. Instrum. **11**, 425–446 (1981)
15. Hsu, C.S., Qian, K., Chen, Y.C.: An innovative approach to data analysis in hydrocarbon characterization by on-line liquid chromatography-mass spectrometry. Anal. Chim. Acta. **264**, 79–89 (1992)
16. Pourshahian, S.: Mass defect from nuclear physics to mass spectral analysis. J. Am. Soc. Mass Spectrom. **28**, 1836–1843 (2017)
17. Fouquet, T., Sato, H.: Convenient visualization of high-resolution tandem mass spectra of synthetic polymer ions using Kendrick mass defect analysis—the case of polysiloxanes. Rapid Commun. Mass Spectrom. **30**, 1361–1364 (2016)
18. Fouquet, T., Nakamura, S., Sato, H.: MALDI Spiral-TOF high resolution mass spectrometry and Kendrick mass defect analysis applied to the characterization of poly(ethylene-co-vinyl acetate) copolymers. Rapid Commun. Mass Spectrom. **30**, 973–981 (2016)
19. Fouquet, T., Aizawa, H., Sato, H.: Taking MALDI Spiral-TOF high resolution mass spectrometry and mass defect analysis to the next level with ethylene vinyl acetate vinyl alcohol terpolymers. Rapid Commun. Mass Spectrom. **30**, 1818–1822 (2016)
20. Fouquet, T., Mertz, G., Delmee, M., Becker, C., Bardon, J., Sato, H.: The definitive evidence of a plasma copolymerization of alkyl and perfluorinated acrylates using high resolution mass spectrometry and mass defect analysis. Plasma Process. Polym. **13**, 862–868 (2016)
21. Fouquet, T., Torimura, M., Sato, H.: Multi-stage mass spectrometry of poly(vinyl pyrrolidone) and its vinyl succinimide copolymer formed upon exposure to sodium hypochlorite. Mass Spectrom. (Tokyo). **5**, A0050 (2016)
22. Fouquet, T., Sato, H.: Improving the resolution of Kendrick mass defect analysis for polymer ions with fractional base units. Mass Spectrom. (Tokyo). **6**, A0055 (2017)
23. Fouquet, T., Sato, H.: How to choose the best fractional base unit for a high resolution Kendrick mass defect analysis of polymer ions. Rapid Commun. Mass Spectrom. **31**, 1067–1072 (2017)
24. Fouquet, T., Shimada, H., Maeno, K., Ito, K., Ozeki, Y., Kitagawa, S., Ohtani, H., Sato, H.: High-resolution Kendrick mass defect analysis of poly(ethylene oxide)-based non-ionic surfactants and their degradation products. J. Oleo Sci. **66**, 1061–1072 (2017)
25. Fouquet, T., Sato, H.: Extension of the Kendrick mass defect analysis of homopolymers to low resolution and high mass range mass spectra using fractional base units. Anal. Chem. **89**, 2682–2686 (2017)
26. Charles, L.: MALDI of synthetic polymers with labile end-groups. Mass Spectrom. Rev. **33**, 523–543 (2014)
27. Gruendling, T., Weidner, S., Falkenhagen, J., Barner-Kowollik, C.: Mass spectrometry in polymer chemistry: a state-of-the-art up-date. Polym. Chem. **1**, 599–617 (2010)
28. Pasch, H., Schrepp, W.: MALDI-TOF Mass Spectrometry of Synthetic Polymers. Springer-Verlag, Berlin (2003)
29. Chendo, C., Charles, L.: Generation of doubly charged species from small synthetic polymers in a high pressure MALDI source. Int. J. Mass Spectrom. **416**, 46–52 (2017)
30. Karas, M., Glückmann, M., Schäfer, J.: Ionization in matrix-assisted laser desorption/ionization: singly charged molecular ions are the lucky survivors. J. Mass Spectrom. **35**, 1–12 (2000)
31. Cody, R.B., Fouquet, T.: Paper spray and Kendrick mass defect analysis of block and random ethylene oxide/propylene oxide copolymers. Anal. Chim. Acta. **989**, 38–44 (2017)
32. Chan, K.W.S., Cook, K.D.: Extended mass range by multiple charge: sampling quadruply charged quasimolecular ions of poly(ethylene glycol) 4000. J. Mass Spectrum. **18**, 423–425 (1983)
33. Fouquet, T., Satoh, T., Sato, H.: First gut instincts are always right: the resolution required for a mass defect analysis of polymer ions can be as low as oligomeric. Anal. Chem. **90**, 2404–2408 (2018)
34. Fouquet, T., Cody, R.B.: Capabilities of the remainders of nominal Kendrick masses and the referenced Kendrick mass defects for copolymer ions. J. Mass Spectrom. **52**, 618–624 (2017)